SOILS AND FOUNDATIONS Vol. 48, No. 6, 805–819, Dec. 2008
Japanese Geotechnical Society

A SLOPE STABILITY ANALYSIS CONSIDERING UNDRAINED STRENGTH ANISOTROPY OF NATURAL CLAY DEPOSITS

Takaharu Shogaki[i] and Naohisa Kumagai[ii]

ABSTRACT

The effects of sites and plasticity index (I_p) on the inherent strength anisotropy of eleven different clay deposits are quantitatively examined by the unconfined compression test using a small size specimen with a different angle of inclination to the vertical. A new method for a slope stability analysis, taking the effects of the IASIA method (Inherent And Stress Induced Anisotropies) into consideration, is proposed. The applicability of the IASIA method and the optimum embankment design are examined through case histories of embankment failures on soft soils. The undrained strength anisotropy cannot be estimated by parameters such as the I_p value because of the complicated relationship with the factors influencing undrained anisotropic strength. It must be directly measured. The IASIA method was recommended from a study of a failed embankment. The probability of failure (P_f) and consumer's risk (P_c) from half of the unconfined compressive strength ($q_u/2$) were $(2.5\sim25.5)$% and $(4.7\sim42.3)$% less than those of the Iwai $q_u/2_{(\mathrm{IASIA})}$ and Urayasu $q_u/2_{(\mathrm{IASIA})}$. Therefore, the design results were underestimated by disregarding strength anisotropies. If, P_f and P_c were considered, the C_t values increased. However, the P_c values drastically decreased to 24.8% from 54.3% concerning the 75-mm sampler and n increased, thus avoiding latent risks. These mean that the IASIA method can be used for optimum embankment design based on performance provisions.

Key words: clay, consumer's risk, embankment design, organic soil, performance-based design, probability of failure, sample disturbance, slope stability analysis, strength anisotropy, total cost, undrained shear strength (**IGC**: C6/C8/D5/H6)

INTRODUCTION

Undrained shear strength anisotropies in soils are classified by the inherent and stress induced anisotropies. Casagrande and Carrilo (1944) determined that the inherent anisotropy is caused by the fabric anisotropy of sedimented soil particles and the stress-induced anisotropy is caused by the anisotropic stress history after sedimentation.

To increase the reliability of designs for slope stability and deformation analyses, it is necessary to develop an analytical method taking into consideration the soil anisotropies. For the deformation analysis, a system of settlement analysis, taking into consideration both anisotropy and disturbance in soil improved by vertical drain, was developed by Shogaki et al. (1998). On the other hand, to evaluate the inherent strength anisotropy of soils for slope stability analysis, various experimental studies have been performed by many researchers, such as Lo (1965), Aas (1965), Bjerrum (1973) and Mikasa et al. (1987), etc.

Lo (1965) performed the unconfined compression test on specimens, 38 mm in diameter (d) and 75 mm in height (h), with a different angle of inclination (β) to the vertical for the Welland and Ontario clays obtained from block sampling and he showed that the ratios of unconfined compressive strength (q_u) for specimens with $\beta=90°$ to those of specimens with $\beta=0°$ ($q_u(90°)/q_u(0°)$) are in the range of 0.64 to 0.80. Aas (1965) measured the undrained strength anisotropy using the vane test of various shapes. Bjerrum (1973) showed that the ratios of the triaxial extensive strength to the triaxial compressive strength after K_0-consolidation under the effective overburden pressure (σ'_{vo}), for samples obtained from six different natural deposit clays, are in the range of 0.18 to 0.73. Mikasa et al. (1987) showed, from a series of unconsolidated undrained direct shear tests on clays consolidated one-dimensionally in laboratory, that the maximum and minimum shear strength took place in the active and passive shear respectively, on a shear plane of $\beta=45°$.

For the studies mentioned above, the following differences in practices can be pointed out. Regarding the unconfined compression test for the specimens, 38 mm in diameter and 75 mm in height, as shown by Lo (1965), specimens with different β can not be made from the 75 mm sampler, which is widely used in Asian countries. The vane test does not reflect the shear condition of the actual failure and the triaxial test cannot measure the strength

i) Associate Professor, Department of Civil and Environment Engineering, National Defense Academy, Japan (shogaki@nda.ac.jp).
ii) Graduate Student, ditto.
The manuscript for this paper was received for review on May 15, 2008; approved on October 10, 2008.
Written discussions on this paper should be submitted before July 1, 2009 to the Japanese Geotechnical Society, 4-38-2, Sengoku, Bunkyo-ku, Tokyo 112-0011, Japan. Upon request the closing date may be extended one month.

under general stress conditions, except for axisymmetric compression and extension. The direction of the confining pressure of the direct shear test for specimens with different β differs from the vertical direction of the *in-situ* condition as shown in Fig. 1.

Measurement of the strength anisotropy using an ordinary sample obtained from the vertical direction would be advantageous. There is no difference in shear strength characteristics between small size specimens (S specimen) with $d=15$ mm and O (or Ordinary size) specimens with $d=35$ mm, which were examined for soils with plasticity indexes (I_p) and q_u in the range of 10 to 370 and 18 kPa to 1000 kPa, respectively (Shogaki, 2007). The S specimen prepared from the ordinary tube sampler can indicate the undrained strength anisotropy in specimens with different β using the unconfined compression test. The methods for slope stability analysis, taking the effect of the inherent strength anisotropy, are proposed by Lo (1965), etc. However, these methods for slope stability analysis cannot evaluate the effect of the stress-induced anisotropy.

In this paper, the undrained strength anisotropies of the Holocene marine clay deposits are examined by unconfined compression tests using S specimens and a portable unconfined compression test apparatus (Shogaki, 2007). The effect of the inherent strength anisotropy on sites and I_p is quantitatively examined. A new method for a slope stability analysis taking into consideration both the inherent and the stress-induced anisotropies (IASIA) is also proposed. Finally, the effects of the anisotropy on the safety factor (F_s) of the conventional $\phi_u=0$ circular slip surface method and the optimum embankment design are examined through case histories of embankment failures on soft soils using the IASIA method.

SOIL SAMPLES

The undisturbed soil samples used in this study were obtained from Holocene marine clays located at ten

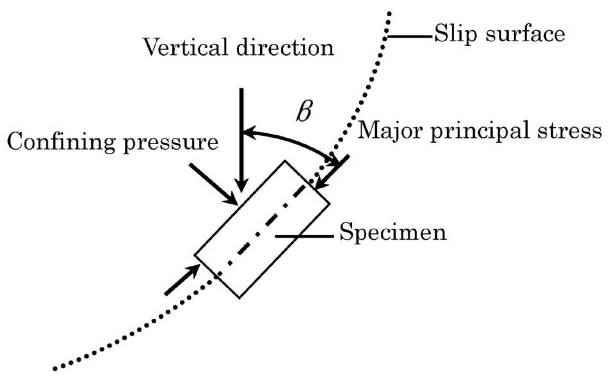

Fig. 1. Relationship between the directions of confining pressure and vertical for direct shear test specimen

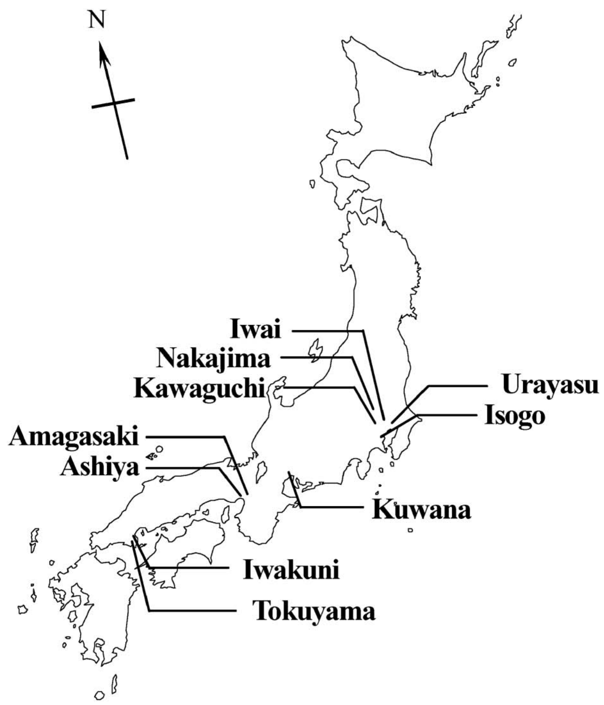

Fig. 2. Sampling site

Table 1. The index, strength and consolidation properties

Site	w_L (%)	I_P (%)	CC^* ($-2\,\mu$%)	q_u (kPa)	σ'_p (kPa)	σ'_{vo} (kPa)	OCR (σ'_p/σ'_{vo})
Amagasaki	45 ~ 102	22 ~ 63	30 ~ 54	121 ~ 164	177 ~ 280	184 ~ 259	0.8 ~ 1.5
Ashiya	96 ~ 111	59 ~ 71	32 ~ 42	23 ~ 57	29 ~ 86	51 ~ 92	0.6 ~ 0.9
Isogo	64	31	32	106	137	120	1.1
Iwakuni	61 ~ 85	30 ~ 49	22 ~ 45	97 ~ 132	90 ~ 194	83 ~ 173	1.1
Iwai	67 ~ 655	34 ~ 370	23 ~ 63	9 ~ 63	11 ~ 48	14 ~ 23	1.0 ~ 2.5
Kawaguchi	53	31	20	23 ~ 80	146	75	2.0
Kuwana	53 ~ 100	27 ~ 42	3 ~ 30	72 ~ 337	133 ~ 255	98 ~ 198	1.1 ~ 1.3
Nakajima	46	3	10	37 ~ 73	150	14 ~ 33	1.8
Tokuyama	33 ~ 138	19 ~ 96	36 ~ 42	27 ~ 113	11 ~ 111	9 ~ 54	1.2 ~ 2.1
Urayasu	47 ~ 114	27 ~ 65	50 ~ 52	96 ~ 174	185 ~ 538	148 ~ 157	1.2

CC^*: Clay composition of less than 2 μm different sites in Japan. Field sampling was performed with 75 mm and 45 mm stationary piston samplers to enhance the quality of the samples. For the Japanese soft clays, these samplers give a quality similar to that sampled by the Laval type sampler (Tanaka et al., 1996).

The sites and index properties of these soils are shown in Fig. 2 and Table 1. These are saturated soils from the Kantoh to the Chugoku regions in Japan. The I_p is 3 to 370, the q_u value is 23 kPa to 337 kPa and the OCR ($=\sigma'_p/\sigma'_{vo}$) value is 0.6 to 2.5. The OCR values for the Amagasaki and the Ashiya clays are below 1.0 because the consolidation of these clays under a reclamation load has not yet been completed.

A METHOD FOR MEASUREMENT OF INHERENT ANISOTROPY ON UNDRAINED SHEAR STRENGTH

To investigate the inherent anisotropy on undrained shear strength, S specimens with different β were taken from samples 75 mm in diameter and 100 mm in height as shown in Fig. 3. The specimen in Fig. 3 is a few mm away from the tube wall. It had been previously confirmed that the stress-strain curves of all ten S specimens taken from samples 75 mm d and 45 mm h were similar (Shogaki et al., 1995a).

Using the scanning electron microscope, Shogaki and Matsuo (1985) and Shogaki (2006a) examined the effect of micro structural disturbance caused by the penetration of the sampling tube and the extrusion of soil samples. For undisturbed Yokkaichi clay with $I_p=44$ obtained by the 75 mm stationary piston sampler, there was complete remolding at the tube wall, but 2 mm from the wall, the microstructure was similar to that at the center of the tube (Shogaki and Matsuo, 1985).

The statistical properties of soil data within thin walled samplers of Holocene marine clay deposits were investigated by an unconfined compression test using an S specimen (Shogaki et al., 1995a; Shogaki, 2007). Regarding the stationary piston sampler 75 mm in inner diameter and 1000 mm in length, which is widely used in Japan, the range of sample disturbance caused by the penetration of the sampling tube and the extrusion of soil samples is within about 2 mm of the wall of the sampling tube. The effect of sample disturbance with thin walled samplers is small, in the range of 100 ~ 600 mm from the cutting edge of the sampling tube. The values of coefficient of variation for q_u are in the range of 0.04 to 0.12. These values are similar to that of reconsolidated clay in Holocene marine clay and are smaller than 0.16 to 0.28 for those of Holocene marine clay deposits (Matsuo and Shogaki, 1988).

These results show the validity of measurement of the inherent anisotropy on undrained shear strength from the specimens, as shown in Fig. 3. This method for measurement of inherent anisotropy is useful because it can be done from samples taken with the stationary 75 mm piston sampler, which is also widely used in Asian countries.

In the unconfined compression test, the specimens were sheared at a strain rate of 1%/min with the portable unconfined compression apparatus (Shogaki, 2007). The value of q_u was determined to be the maximum stress corresponding to an axial strain (ε_a) of less than 15%. The secant modulus (E_{50}) is given by $q_u/2\ \varepsilon_{50}$, in which ε_{50} is the strain at the value of $q_u/2$. The $\bar{q}_u$, $\bar{E}_{50}$ and the strain at failure ($\bar{\varepsilon}_f$) are mean values of q_u, E_{50} and ε_f.

EFFECTS OF SITE AND I_p ON INHERENT ANISOTROPY OF UNDRAINED SHEAR STRENGTH

The stress-strain curves for specimens with $\beta=0°$, 30°, 60° and 90° for the Kuwana clay with $I_p=52$ are shown in Fig. 4. The q_u values and the initial tangent modulus decreases and the ε_f values increase as the β values increase. These tendencies are independent of the site, I_p and q_u of sample, and are also similar to that reported by Lo (1965), Duncan and Seed (1966a) and Mikasa et al. (1987).

The ratios of the $\bar{q}_u$ values of specimens at various β to those of specimens with $\beta=0°$ ($\bar{q}_u(\beta)/\bar{q}_u(0°)$) are plotted against the β values in Fig. 5. The ratios of $\bar{q}_u(\beta)/\bar{q}_u(0°)$ in Fig. 5 decrease with the increase in the β values and the

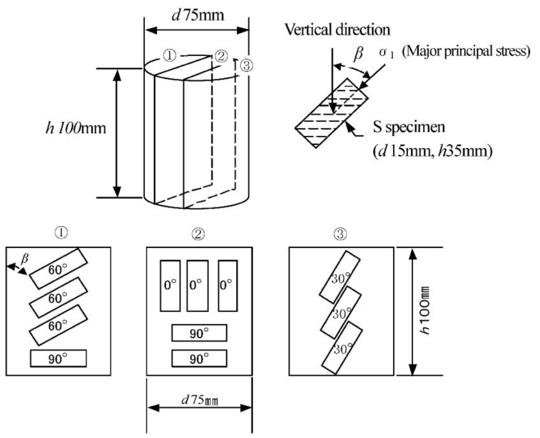

Fig. 3. Site location where soil specimens were obtained

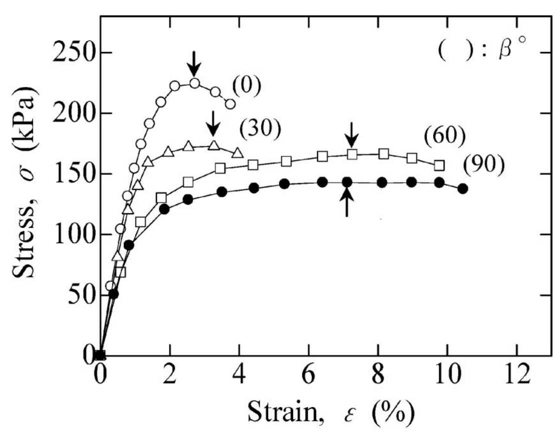

Fig. 4. The relationship between stress and strain (Kuwana clay)

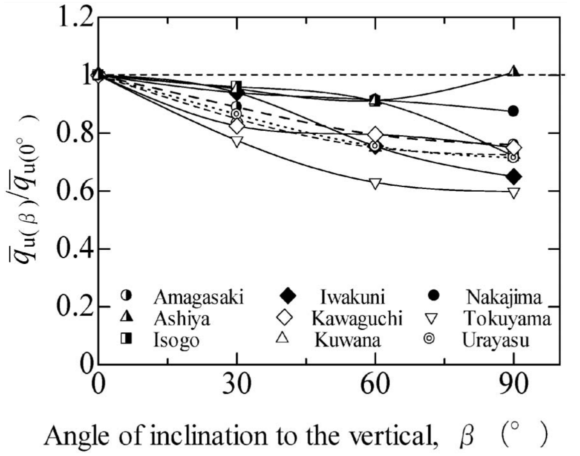

Fig. 5. The relationship between $\bar{q}_u(\beta)/\bar{q}_u(0°)$ and β

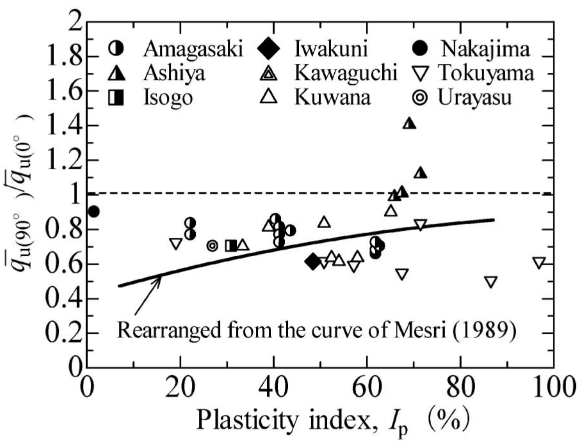

Fig. 6. The relationship between $\bar{q}_u(\beta)/\bar{q}_u(0°)$ and I_p

values of $\beta=90°$ are consistently smaller. For Ashiya clay, the $\bar{q}_u(\beta)/\bar{q}_u(0°)$ values are about 1.0. The anisotropy of the q_u value weakens by about fifty percent for the undisturbed q_u values that decrease the undrained shear strength (Shogaki et al., 1995b). The consolidation of Ashiya clay under a reclamation load has not yet been completed. The undrained shear strength anisotropy weakened because the soil structure was deformed by excess pore water pressure caused by a reclamation load.

In the case of Tokuyama and Iwakuni clays, the $\bar{q}_u(90°)/\bar{q}_u(0°)$ values are about 0.60 and 0.65 respectively, and smaller than those of other sites. This means that the inherent anisotropy on the undrained shear strength of the soils in the design area must be directly measured because it varies by site.

The relationship between the $\bar{q}_u(90°)/\bar{q}_u(0°)$ values and the I_p values is shown in Fig. 6. The $\bar{q}_u(90°)/\bar{q}_u(0°)$ values are in the range of 0.5 to 0.9 except for Ashia clay. The solid line in Fig. 6 shows the ratio obtained by rearranging the curve for the triaxial extensive strength and the triaxial compressive strength of the natural deposit soils measured by Mesri (1989). Bjerrum (1973) and Ladd et al. (1977) showed that the ratio of triaxial extensive strength to the triaxial compressive strength decreases with a decrease in the I_p value. The data shown in Fig. 6 show a dissimilar tendency to the solid line and appear to be independent of the I_p values.

Hanzawa and Tanaka (1992) showed that the ratios of triaxial extensive strength to the triaxial compressive strength for the Japan, Indonesia and Arabian clays are constant for the I_p values. The results given from the q_u values with different β coincide with the result by Hanzawa and Tanaka (1992).

The undrained strength anisotropy cannot be estimated by parameters such as the I_p value because of the complicated relationship with the factors influencing undrained anisotropic strength.

A NEW METHOD FOR SLOPE STABILITY ANALYSIS, TAKING THE EFFECTS OF INHERENT AND STRESS INDUCED ANISOTROPIES INTO CONSIDERATION

A Review of Methods for Slope Stability Analysis, Taking the Effect of Anisotropy into Consideration

A constitutive equation of soils, taking the effect of induced anisotropy and time dependency in clays into consideration, was developed by Sekiguchi and Ohta (1977). Asaoka and Kodaka (1992) proposed a solution for solving the soil-water coupling problems, in which stress induced strength anisotropy used the rigid plastic finite element method. The $\phi_u=0$ circular slip surface method has been widely used in practice as a slope stability analysis on saturated clay deposits. For the $\phi_u=0$ circular slip surface method in Japan, the $q_u/2$ value has been adopted as a resistant strength mobilized on the circular slip surface. It was pointed out by Duncan and Seed (1966a) that the shear strength mobilized on the failure surface varies with the orientation of the major principal stress on the circular slip surface because the natural clay deposits have anisotropy caused by the depositional environment and stress histories, as explained in the previous chapter.

Lo (1965), Bishop (1966), Davis and Christian (1971) and Mikasa et al. (1987) plotted the undrained strength from unconfined compression tests for the specimens with various β against a polar diagram of undrained shear strength (c_u) and β values and estimated the inherent anisotropy on the c_u by interpolating these plots to an elliptical curve. Lo (1965) proposed a method for slope stability analysis, taking the effect of the inherent strength anisotropy into consideration, based on estimating the undrained anisotropic strength to the elliptical curve in the polar diagram. For heavily consolidated and varied clays (Ladd et al., 1977), this method of estimating inherent strength cannot be used due to the constant inability of the $\beta=45°$ value to fit into a continuous elliptical curve.

Regarding soft soil, the slow construction method with vertical drain is adopted frequently because of the effect of the expected increase of shear strength caused by consolidation. For stability problem designs in these types of soils, the strength increase is generally evaluated by the

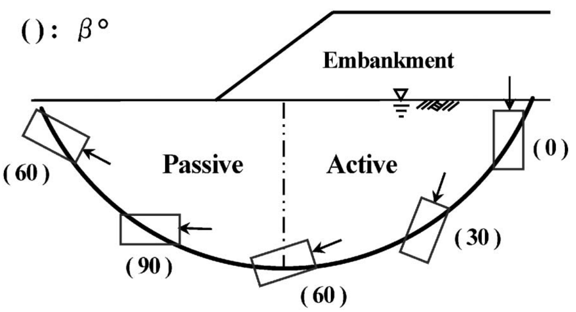

Fig. 7. Schematic representation of the layout of anisotropy on the circular slip surface

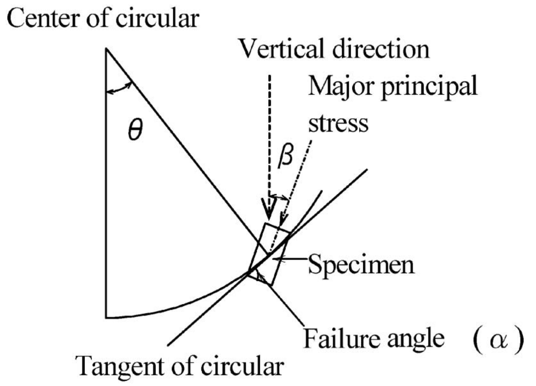

Fig. 8. Definition of geometric parameters of θ and β

rate of strength increase (c_u/p) obtained from the triaxial tests for the soils in the design. The effect of anisotropy on the c_u/p value is not considered.

A Method for Slope Stability Analysis, Taking the Effect of Inherent Anisotropy on the Undrained Strength into Consideration

A schematic representation of the layout of the inherent strength anisotropy on the circular slip surface is shown in Fig. 7. At any point along any potential failure surface, the inherent anisotropic strength is obtained from the failure angle (α) of a specimen to make the circular slip surface consistent. The q_u values on the circular slip surface correspond to the q_u values with $\beta = 60°$ at the bottom, $\beta = 0° \sim 60°$ in the region of active earth pressure and in the $\beta = 60° \sim 90°$ in the region of passive earth pressure. Figure 8 shows the definition of the geometric parameters of both the vertical angle of circular slip surface (θ) and the β value. The angle θ is defined geometrically as Eq. (1).

$$\theta = \alpha - \beta \tag{1}$$

where the α value can be fixed at 60°. This validity was discussed in the authors' other papers (Shogaki and Moro, 1996).

A method for slope stability analysis, taking the inherent strength anisotropy on the undrained strength into consideration, can be performed by including the inherent anisotropic strength at any point along any potential failure surface described above in the conventional $\phi_u = 0$ circular slip surface method. This method does not have the faults of the elliptical curve in the polar diagram by Lo (1965).

A Method for Slope Stability Analysis, Taking the Effects of the Inherent and Stress Induced Anisotropies on the Undrained Strength into Consideration

Hansen and Gibson (1949) derived the equations on the c_u/p value, taking the orientation of the major principal stress under the undrained and the plane strain conditions into consideration. The Skempton's λ theory (Skempton, 1948) and Hvorslev's strength parameters (Hvorslev, 1960) were used in these equations. These equations are not convenient in practice because the λ theory and these strength parameters are very difficult to analyze. To solve this problem, Duncan and Seed (1966b) modified Hansen and Gibson's equations (1949) using the pore water pressure coefficient (A) by Skempton (1954) and the effective cohesion (c') and the effective angle of friction (ϕ') and they derived Eq. (2), which is useful in practice.

$$\left(\frac{c_u}{p}\right)_\theta = \frac{c'}{p}\cos\phi' + \frac{1}{2}(1+K_0)\sin\phi' - \sin\phi'(2A_{f(\theta)}-1) \times \left\{\left(\frac{c_u}{p}\right)^2 - \frac{c_u}{p}(1-K_0)\cos 2\left(45° + \frac{\phi'}{2} - \theta\right) + \left(\frac{1-K_0}{2}\right)^2\right\}^{1/2} \tag{2}$$

where $(c_u/p)_\theta$ is the rate of strength increase on θ, and A_f pore water pressure coefficient at failure. Duncan and Seed (1966b) also gave the A_f value ($A_{f(\theta)}$) with the orientation of the major principal stress as Eq. (3).

$$A_{f(\theta)} = A_{f(\min)} + (A_{f(\max)} - A_{f(\min)})\sin^2(\theta + 30°) \tag{3}$$

where the $A_{f(\max)}$ and $A_{f(\min)}$ values are the A_f value for which the directions of the major principal stress are vertical and horizontal, respectively. The c_u/p values with the anisotropy of the A_f value can be evaluated using Eqs. (2) and (3).

The stress-induced anisotropy on the undrained shear strength is obtained by piling the inherent anisotropy. The resistance moments, which make allowance for the inherent and stress induced anisotropy, are given as M_r(i) and M_r(s), respectively in Eq. (4).

$$M_r = M_{r(i)} + M_{r(s)} = \int f(\theta)(c_0 + kz)R^2 d\theta + \int \left\{\left(\frac{c_u}{p}\right)_\theta \Delta p U\right\} R^2 d\theta \tag{4}$$

where $f(\theta)$ is the coefficient of inherent anisotropic strength at various θ as shown in Fig. 8, c_0 the undrained strength at ground surface, k the strength increase coefficient for depth (z), Δp the increment of embankment load, U the degree of consolidation, and R the radius of circular.

A method for the slope stability analysis, taking the effects of the IASIA method (Inherent And Stress Induced Anisotropies) into consideration, can be performed by using Eq. (4) as the resistance moment to the conventional $\phi_u=0$ circular slip surface method.

APPLICABILITY OF THE IASIA METHOD

In this section, the effect of the anisotropic strength on the F_s value of the conventional $\phi_u=0$ circular slip surface method is examined through case histories of embankment failures on soft soils using the IASIA method.

It is well known that the conventional $\phi_u=0$ circular slip surface method has many factors influencing the F_s value and it is highly accurate for design results because these factors are canceled out in total (Matsuo and Asaoka, 1976). The coefficient for each factor has been proposed by many researchers, such as Asaoka and Ohtsuka (1989), Tsuchida et al. (1989) and Hanzawa (1995), etc.

Asaoka and Ohtsuka (1989), using the slope stability, pointed out anisotropy, plane strain, overconsolidation of ground surface and strength increase as the four factors in the strength of the slip surfaces and gave the coefficient for these factors analytically using the Cam-clay model and Sekiguchi-Ohta's constitutive equation (Sekiguchi and Ohta, 1977). The mobilized undrained shear strength (c_u(mob)) for the slope stability is expressed as Eq. (5).

$$c_u(\text{mob})=\mu_R\times\mu_A\times\mu_S\times\mu_C\times q_u/2 \qquad (5)$$

where the μ_R is the coefficient for the strain rate, μ_A the coefficient for the strength anisotropy, μ_S the coefficient for the sample disturbance and μ_C the coefficient for the release of *in-situ* stress. Asaoka and Ohtsuka (1989) showed the c_u(mob) to be equal to $q_u/2$ because the four coefficients in Eq. (5) are canceled out and become 1.0.

Tsuchida et al. (1989) pointed out six factors of the slip surface strength as strain rate, anisotropy, the release of *in-situ* stress, sample disturbance, plane strain, and the strength of $\alpha=45°$, regardless of $\alpha=60°$. The effects of plane strain and the strength of $\alpha=45°$ can be ignored because these factors are canceled out. Tsuchida et al. (1989) expressed the c_u(mob) value as Eq. (6).

$$c_u(\text{mob})=\mu_R\times\mu_A\times c_u(c)=0.75\ c_u(c) \qquad (6)$$

where the $c_u(c)$ is the triaxial compressive strength from the strain rate of 0.2%/min after isotropic consolidation under $2/3\sigma'_{vo}$. Hanzawa (1995) proposed a method of slope stability analysis using the strength of the direct shear test. Hanzawa (1995) expressed the c_u(mob) value as Eq. (7).

$$c_u(\text{mob})=\mu_R\times c_u(\text{D})=0.85\ c_u(\text{D}) \qquad (7)$$

In this method, the effect of the μ_A, μ_C, μ_S and plane strain are not considered because the c_u(D) value comes from the direct shear test after K_0-consolidation.

The relationship between the q_u value and the c_u(C), c_u (D) values therefore, are shown as Eqs. (8), (9) from Eqs. (5), (6) and (7), respectively.

$$c_u(\text{C})=\mu_S\times\mu_C\times q_u/2 \qquad (8)$$
$$c_u(\text{D})=\mu_A\times\mu_S\times\mu_C\times q_u/2 \qquad (9)$$

Table 2. Coefficient for factors influencing mobilized undrained shear strength

The factors influencing F_s		Methods		
		Asaoka	Tsuchida	Hanzawa
Strain rate	μ_R	—	0.88	0.85
Anisotropy	μ_A	0.69	0.85	1.00[3)]
Release of *in-situ* stress	μ_C	—	1.33[1)]	1.00[4)]
Sample disturbance	μ_S	—	1.33[1)]	1.00[4)]
$\alpha=60°$	μ_α	—	1.00[2)]	—
Plain strain	μ_P	1.15	1.00[2)]	—
Overconsolidation at ground surface	μ_O	1.13	—	—
Increase in shear strength	μ_I	1.12	—[5)]	—[5)]

1) The coefficients, which put the effects of release of *in-situ* stress and sample disturbance together, are 1.33. ($\mu_c\times\mu_S=1.33$)
2) The effects of plane strain and $\alpha=60°$ cancel each other out. ($\mu_\alpha\times\mu_P=1.00$)
3) This coefficient is 1.00, because the shear strength obtained from the direct shear test takes anisotropy into consideration.
4) These factors are eliminated by K_0-consolidation.
5) The effect of the increase in shear strength is taken into consideration in design.

The values of coefficient for these factors proposed by Asaoka and Ohtsuka (1989), Tsuchida et al. (1989) and Hanzawa (1995) are listed in Table 2. By using each coefficient shown in Table 2, the conventional, the Asaoka and Ohtsuka (1989), the Tsucida et al. (1989), the Hanzawa (1995) and the IASIA method are all applied to the case histories of embankment failures. The conventional method is the $\phi_u=0$ circular slip surface method using the measured q_u value. In the IASIA method, the inherent anisotropic strength used Urayasu sites as an average example in Fig. 5 because it had not been measured in the case histories sites and the other coefficients used the values shown in Table 2. Coefficients of μ_A, μ_C, μ_S, except the strain rate in the Hanzawa method (1995), used the values for the coefficients in the Tsuchida method (1989).

The site of the embankments used for the case histories are located in Iwamizawa in Hokkaido prefecture (Japan Highway Public Corporation, 1977), Funako in Kanagawa prefecture (Japan Highway Public Corporation, 1966), Fukuroi in Shizuoka prefecture (Yamamoto and Hoshi, 1967), Kohda in Aichi prefecture (Muromachi and Watanabe, 1962), and Kure in Hiroshima prefecture (Adachi and Miyahara, 1962). It was confirmed by these papers that all the embankments except Funako failed. The undrained shear strength used in the stability analysis was figured from the q_u values measured by the unconfined compression test before reclamation.

The F_s values of each stability method are plotted versus each site in Fig. 9. In this figure, the Asaoka and Ohtsuka (1989) and the conventional methods give the same F_s values for each site since the c_u(mob) values are the same. The Hanzawa, Tsuchida and IASIA methods also give similar F_s values for each site. Based on that, it

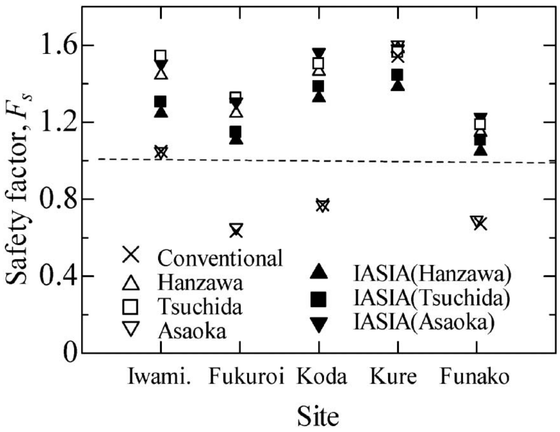

Fig. 9. F_s values of each stability method

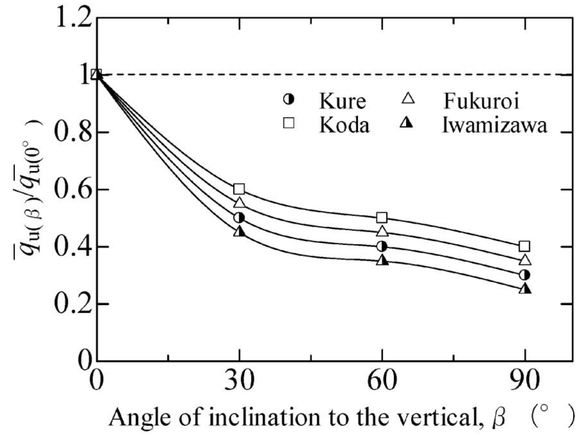

Fig. 10. Strength anisotropy by back analysis

can be concluded that the IASIA method gives a similar strength isotropy to the Hanzawa (1995) and Tsuchida et al. (1989) methods. The F_s values from the Hanzawa, Tsuchida and IASIA methods however, are more than 1.0 and disagree with the actual conditions in which these embankments failed. The reasons considered are as follows:

1) The IASIA methods are calculated using the values of coefficient for plane strain of each method to Eq. (2) since the design harmony is maintained in each method. Asaoka and Otsuka (1989) reported that the shear strength under axisymmetric 15% increase takes plane strain into account. Therefore, it is considered that the F_s value increases doubling the coefficient of plane strain.
2) In this case study, it is calculated on the assumption that other factors influencing F_s such as progressive failure, three dimensional failure, non-circular slip surface, neglect of friction angle of soils, strength of embankment, etc. compensate for the F_s values. The coefficients of these factors differ by design condition type of embankment failure, embankment shape and materials, etc.
3) In organic soils, it is well known that the strength anisotropy caused by the organic matter content and its fabric is greater than that of inorganic soils (JSSMFE, 1990). In this case study, the evaluation of the anisotropic strengths for organic soils, clay and organic soil layers used the Urayasu site as an average example.

The range of F_s values is from 0.96 to 1.21, a 15% reduction from the values obtained from the IASIA method as shown in Fig. 9. Therefore, the actual conditions in which embankments failed cannot be explained if plane strain as described above is considered. The anisotropic strengths for the soil below the failed embankment are evaluated by back analysis as $F_s = 0.99$. The results are shown in Fig. 10. For Iwamizawa, the strength anisotropy is greater than those of other sites and the $\bar{q}_u(90°)/\bar{q}_u(0°) \fallingdotseq 0.2$ for $\bar{q}_u(90°)/\bar{q}_u(0°) \fallingdotseq 0.6 \sim 0.8$, as shown in Fig. 5. Kohda is the smallest, with a $\bar{q}_u(90°)/\bar{q}_u(0°)$ value of about 0.4. The strength isotropies of organic soils are relative to organic matter content (JSSMFE, 1990). The organic matter contents of Iwamizawa were in the range of 40% to 70% (Japan Highway Public Corporation, 1966), and those of Kohda were about 24% (Muromachi and Watanabe, 1962). This coincides with the results shown in Fig. 10.

The values of coefficient for the strength anisotropy of the failed embankments, which were evaluated by back analysis as $F_s = 0.99$, are in the range of 0.49 to 0.70. These values are quite smaller than those of Tsuchida et al. (1989) methods. For organic soil layers, the values of coefficient for the strength anisotropy, as shown in Table 2, produce a positive result for embankment design. The applicability of the IASIA method is recommended from the examination mentioned above.

OPTIMUM EMBANKMENT DESIGN AT IWAI

Investigation Sites at Iwai and Testing Procedures

The investigation sites are located on the Holocene lowland at Iwai in Ibaraki prefecture. The soil sampling for 3 sites is shown in Fig. 11. The undisturbed soil samples were obtained from the Holocene organic and soft clay deposits using the cone (Shogaki et al., 2004a), 45-mm and 50-mm (Shogaki, et al., 2004a; Shogaki et al., 2004b; Shogaki and Sakamoto, 2004), and 75-mm (JGS-1221, 2003) samplers. The sites are located at the north side of the embankment and 23 m away from the embankment's terminal edge.

The K_0 consolidationed-undrained triaxial compression tests (CK_0UC) were performed according to the standards of the Japanese Geotechnical Society (JGS 0525–1996) with a precision triaxial test apparatus (PTA) (Shogaki and Nochikawa, 2004) using small specimens 15 mm in diameter and 35 mm in height. For K_0 consolidation, the lateral pressure can be controlled by computer in order to keep the K_0-consolidation under an axial consolidation strain rate. The lateral strain of the specimen under K_0 consolidation can be controlled with a degree of accuracy of less than 0.02% for a 15 mm diameter specimen. The backpressure and initial isotropic consolidation pressure before K_0-consolidation were 200 kPa and 10 kPa. The

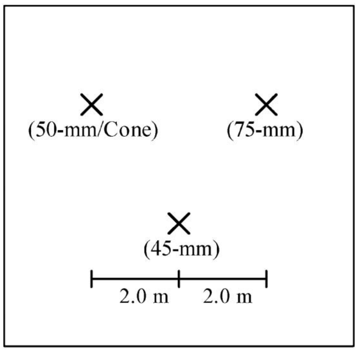

Fig. 11. Sampling site (Iwai site)

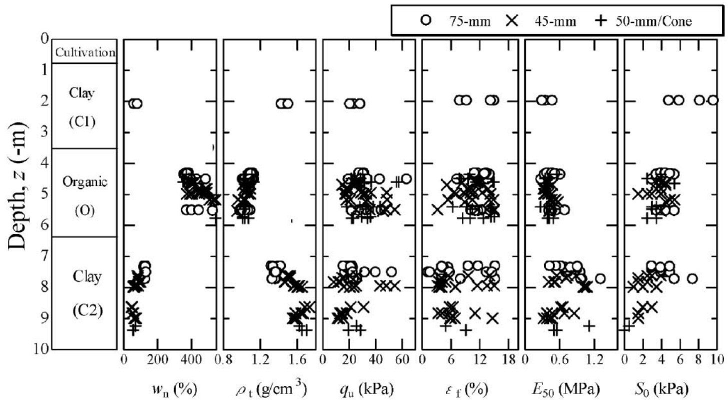

Fig. 12. UCT test results (Iwai soils)

Table 3. The condition and specimen size for the UCT and CK_0UC

Test	Consolidation pressure (kPa)	Strain condition (%/min)	Shear condition	c_u	Specimen size (mm)
UCT	—	1	undrained	$q_u/2$	d15, h35
CK_0UC	10, 20, 30, 40, 50	0.05, 1.0		$q_{max}/2$	

pore pressure coefficient values were greater than 0.98. The UCT used the portable unconfined compression apparatus (PUCA) (Shogaki, 2007). The specimen suction (S_0) for evaluating sample disturbance was measured at the base of the specimen using a ceramic disc plate. The air entry value of a ceramic disc is about 200 kPa. The suction was measured in accordance with the manual for unconfined compression tests with suction measurement (JGS, 2006). The UCT was performed on S specimens at a strain rate of 1%/min after the S_0 was measured. The value of q_u was determined to be the maximum stress corresponding to an axial strain of less than 15%. The secant modulus (E_{50}) is given by $q_u/2\ \varepsilon_{50}$, in which ε_{50} is the strain at the value of $q_u/2$. The condition and specimen size for the UCT and CK_0UC tests are summarized in Table 3.

The oedometer tests were performed using a load increment ratio of unity and the duration of loading for each load increment was one day. The values of the compression index (C_c) and the preconsolidation pressure (σ'_p) were determined from the void ratio (e) to log σ'_v curve based on the Japanese Industrial Standard for determining one-dimensional consolidation properties of soils (JIS A 1217-1993).

Mechanical Properties and Inherent Strength Anisotropies of Iwai Soils

For the actual failed embankment site under construction at Iwai, the mechanical properties and inherent strength anisotropies are measured through the samples obtained from each type of sampler. The sampling depths (z) were (3.5 ~ 6.7) m below the ground surface for organic (O) and (0.7 ~ 3.5) m and (6.7 ~ 9.5) m for clay deposits as shown in Fig. 12. The plasticity index (I_p) values were 199 to 370 and 34 to 63 for organic and clay deposits and these were classified as highly organic and high plasticity clays. The natural water content (w_n), wet density (ρ_t), initial void ratio (e_0), q_u, strain at failure (ε_f), E_{50}, volumetric strain (ε_{vo}), σ'_p, C_c and OCR values obtained from S specimens of samples by the 75-mm, 45-mm, 50-mm and cone samplers for O and soft clay (C2) are plotted against the z in Figs. 13 and 14.

The *in-situ* undrained shear strength ($q_{u(I)}$) was estimated from Shogaki's improved method (2006b) and the *in-situ* undrained shear strength ($c_{u(I)}$) measured from the CK_0UC under the *in-situ* preconsolidation pressure ($\sigma'_{p(I)}$) (Shogaki, 1996) was also estimated. The $q_u/2$, $q_{u(I)}/2$ and $c_{u(I)}$ values obtained from the 75-mm, 45-mm, 50-mm and cone sampler are plotted against the depth in Fig. 15. The C1 clay was sampled only using the 75-mm sampler. The distribution curves and the statistical values of the ratios of undrained shear strength (c_u) are summarized in Figs. 16, 17 and Table 4 and the *in-situ* undrained shear strengths ($c_{u(I)}$) in Table 4 are estimated from CK_0UC under *in-situ* preconsolidation pressure ($\sigma'_{p(I)}$) in Fig. 18 from Shogaki's method (Shogaki, 1996). The ratios of σ'_p to $\sigma'_{p(I)}$ are (67 ~ 79)% and $q_u/2$ to $q_{u(I)}/2$ and $c_{u(I)}$ are (68 ~ 84)% because of sample disturbance.

The stress-strain curves for specimens with $\beta = 0°$, 30°, 60° and 90° for the O and C2 are shown in Figs. 19 and 20. The w_n, ρ_t, S_0, q_u, E_{50} and ε_f values for each specimen are also given in the Figs. 19 and 20 insets. The S_0 value under shear is represented as the pore water pressure (u) in Figs. 19 and 20 since the suction under shear becomes plus, with small S_0 values. Therefore, the u values at the $\varepsilon_a = 0\%$ are S_0 values. The degrees of saturation of specimen were about 100%. The q_u values and the initial tangent modulus decreases and the ε_f values increase with the increase in the β values without regard to similar S_0 values. These tendencies are independent of the soils and depths and are also similar to that reported by Lo (1965), Duncan and Seed (1996b) and Mikasa et al. (1987).

The regression curves for plots of ratios of the q_u values of specimens at various β to those of specimens with $\beta = 0°$ ($q_u(\beta)/\bar{q}_u(0°)$) are shown as solid and broken lines against the β values in Fig. 21. The range for nine different deposits in Japan as shown in Fig. 5 is also shown in Fig. 21. The anisotropic strength of O and C2 deposits

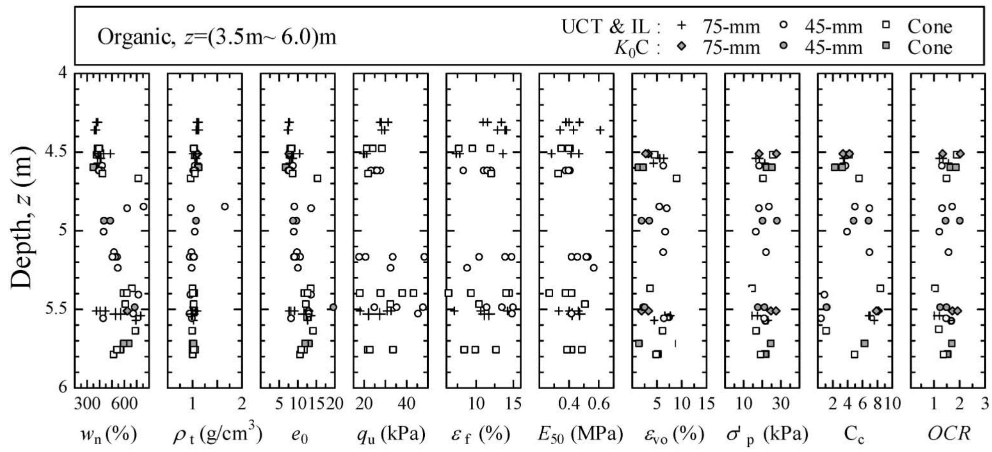

Fig. 13. UCT and IL test results (Organic soil)

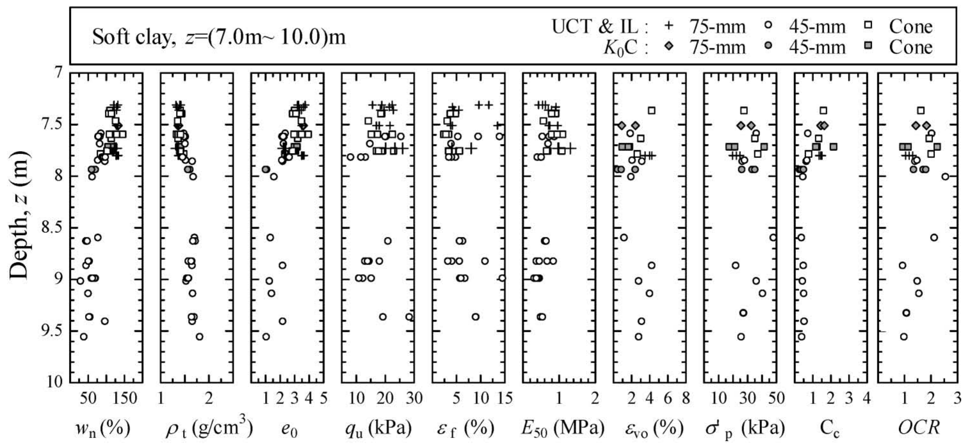

Fig. 14. UCT and IL test results (C2 clay)

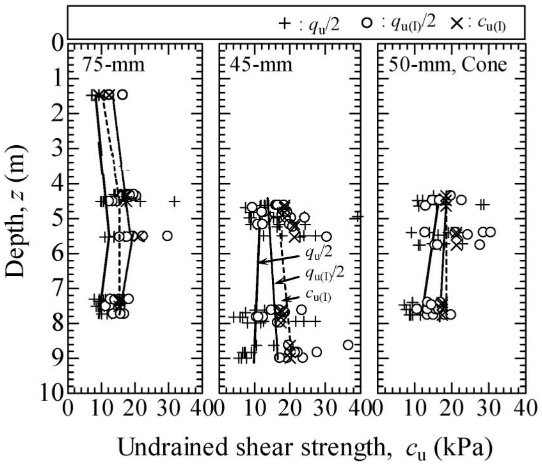

Fig. 15. Undrained shear strength (Iwai soils)

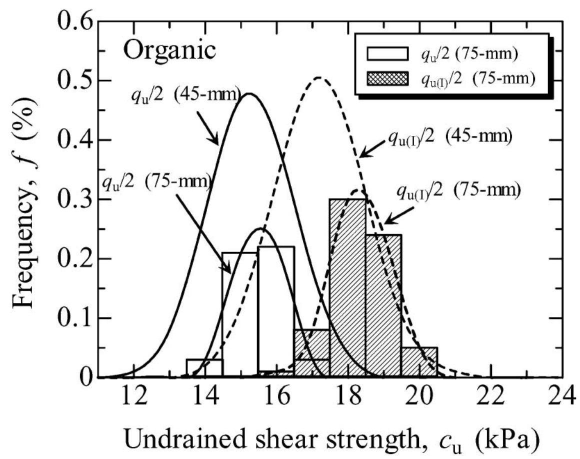

Fig. 16. The distribution curves of undrained shear strength (Organic soil)

are smaller than those of other deposits. In particular, for $\beta = 30°$ and $60°$, the anisotropies are smaller and have isotropic behaviors for c_u. However, the q_u values of $\beta = 90°$ for the O and C2 clay are 71% and 86% of those of $\beta = 0°$. The strength anisotropy caused by the organic matter is also greater than that of inorganic soils at Iwai site. However, the strength anisotropy of the O soil is smaller than those of Iwamizawa, Fukuroi, Koda and Kure as estimated in Fig. 10 since the O soil is classified as muck in which the fiber is ramified. The resolution increased with

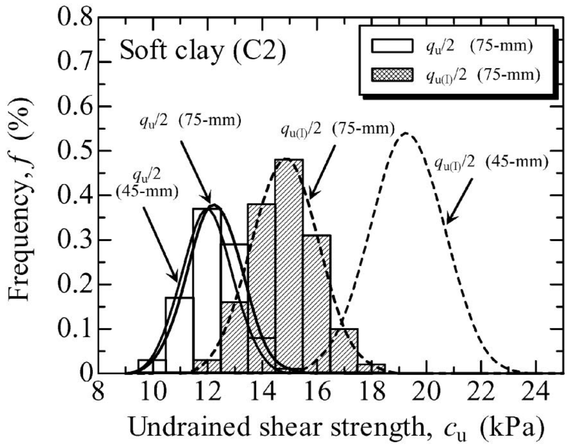

Fig. 17. The distribution curves of undrained shear strength (C2 clay)

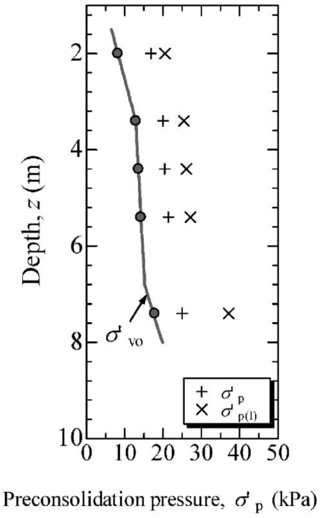

Fig. 18. The effective overburden and preconsolidation pressures (Iwai site)

Table 4. The statistical properties of the undrained shear strength

Soil	Sampler	c_u	n	$\bar{c}_u$ (kPa)	Vc_u
Soft clay (C1)	75-mm	$q_u/2$	4	12.1	0.14
		$q_{u(I)}/2$	4	15.5	0.21
		$c_{u(I)}$	1	12.3	—
Organic (O)	75-mm	$q_u/2$	19	15.5	0.33
		$q_{u(I)}/2$	15	18.4	0.28
		$c_{u(I)}$	2	18.3	0.11
	45-mm	$q_u/2$	26	15.3	0.48
		$q_{u(I)}/2$	17	17.2	0.29
		$c_{u(I)}$	2	19.4	0.07
Soft clay (C2)	75-mm	$q_u/2$	17	12.3	0.51
		$q_{u(I)}/2$	13	14.9	0.11
		$c_{u(I)}$	1	15.3	—
	45-mm	$q_u/2$	27	12.0	0.55
		$q_{u(I)}/2$	19	19.3	0.29
		$c_{u(I)}$	3	20.0	0.16

n: Number of specimen, $\bar{c}_u$: Mean value of c_u, Vc_u: Coefficient of variation of c_u

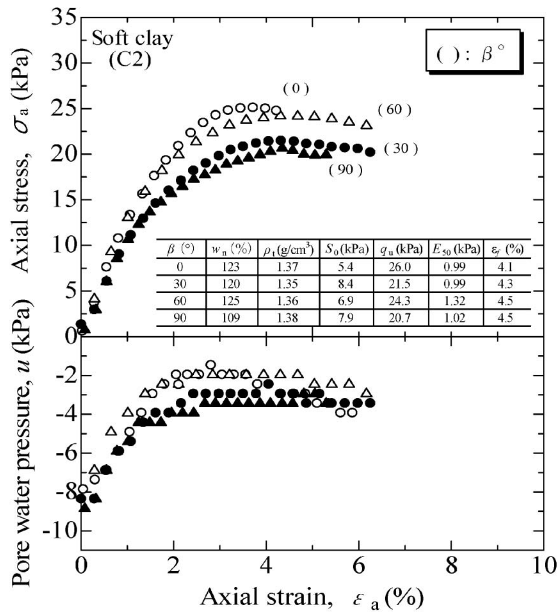

β (°)	w_n (%)	ρ_t (g/cm³)	S_0 (kPa)	q_u (kPa)	E_{50} (kPa)	ε_f (%)
0	123	1.37	5.4	26.0	0.99	4.1
30	120	1.35	8.4	21.5	0.99	4.3
60	125	1.36	6.9	24.3	1.32	4.5
90	109	1.38	7.9	20.7	1.02	4.5

Fig. 19. The relationship between stress and strain (Organic soil)

the ignition loss of (42～73)% and the fiber content (ASTM D4427-92, 1992) of (42～73)% by sieve analysis. There is no proper method for estimating these strength isotropic behaviors, therefore the undrained inherent anisotropic strength of the soils in the designated area must be directly measured. The small size specimens can easily measure the undrained inherent anisotropic strength.

The relationships between the anisotropic strength ($q_{u(I)}/2$(IASIA)) and β using the IASIA method use the measured values shown in Fig. 21. The embankment stability is examined by using c_u obtained from the 75-mm and 45-mm samplers as shown in Table 4. The minimum slip surface safety factors ($F_{s(min)}$) for these c_u are summarized in Table 5. The $F_{s(min)}$ is considered with the traffic load (=9.8 kPa) under embankment construction. The embankment construction site consisted of cultivation, clay (C1) plus the O, C2 and sand layers. The $F_{s(min)}$ for the $q_u/2$ obtained from samplers are smaller than 1.0 and these coincide with embankment failure conditions. The slip surfaces for the $F_{s(min)}$ of the 75-mm sampler are shown in Fig. 22 together with the IASIA method using the anisotropic strength as shown Fig. 21 and the embankment failure condition. The $F_{s(min)}$ values of the $q_u/2$, $q_{u(I)}/2$ and the IASIA method using $q_{u(I)}/2$ are 0.872, 1.039 and 1.016 for the 75-mm sampler since the embankment load is relatively large compared to undrained shear strength of soft soils under embankment. The slip surfaces coincide with the actual failed embankment since the positions of embankment cracks and the heaving surrounding the embankment's toe plus the depth in which the cone penetration force decreased coincide with the slip surfaces. The application of the IASIA method is confirmed from a study of a failed embankment on soft soil.

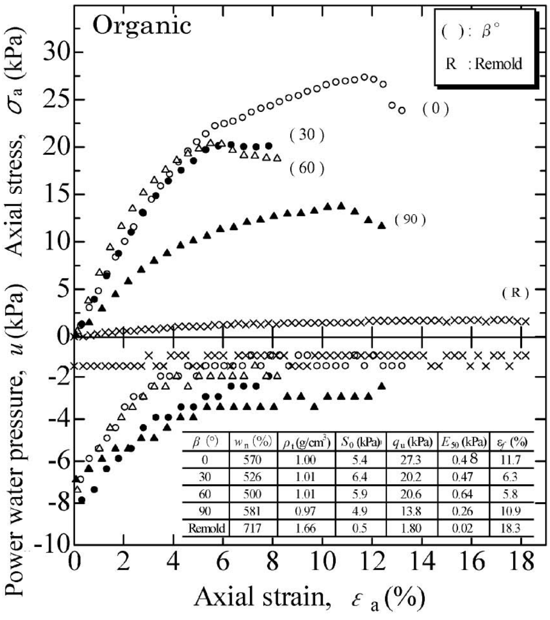

Fig. 20. The relationship between stress and strain (C2 clay)

Effects of Sample Disturbance and Strength Anisotropy on Optimum Embankment Design at the Iwai Site

As described in a previous section, the conventional $\phi_u = 0$ circular slip surface method has many factors influencing the F_s value. In this section, the effects of sample disturbance and strength isotropy on optimum embankment design are quantitatively examined through a study of a failed embankment on soft soils at the Iwai site. The correction of sample disturbance overestimates the F_s value since the undrained shear strength increases with its correction and the strength isotropy is completely opposite. Embankment design reliability can be increased through the examination of these studies for each factor.

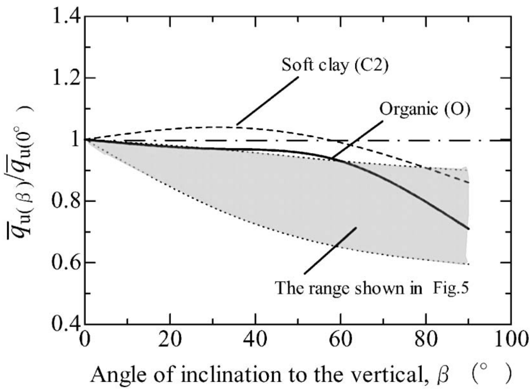

Fig. 21. The relationship between $\bar{q}_u(\beta)/\bar{q}_u(0°)$ and β (Iwai soils)

Table 5. n, $C_{t(min)}$, P_f and P_c values obtained from each c_u (75-mm and 45-mm samplers)

Sampler	Undrained shear strength, c_u	Error consideration	Number of specimen, n	P_f (%)	P_c (%)	$C_{t(min)}$ (K-yen/m)	$F_{s(min)}$
75-mm	$q_u/2$	P_f	200	40.2		1088	0.872
		P_f and P_c	226	39.3	49.6	1169	
	$q_u/2_{(IASIA)}$ (Iwai)	P_f	188	42.8		1105	0.853
		P_f and P_c	219	41.8	54.3	1203	
	$q_u/2_{(IASIA)}$ (Urayasu)	P_f	157	55.2		1194	0.641
		P_f and P_c	30	64.8	91.9	1447	
	$q_{u(I)}/2$	P_f	100	9.8		823	1.039
		P_f and P_c	104	9.7	20.5	908	
	$q_{u(I)}/2_{(IASIA)}$ (Iwai)	P_f	134	13.7		863	1.016
		P_f and P_c	123	14.1	24.8	947	
45-mm	$q_u/2$	P_f	223	34.0		1044	0.863
		P_f and P_c	37	50.3	84.4	1391	
	$q_u/2_{(IASIA)}$ (Iwai)	P_f	245	37.4		1077	0.844
		P_f and P_c	82	47.4	94.4	1481	
	$q_{u(I)}/2$	P_f	27	0.4		730	1.073
		P_f and P_c	75	0.0	1.4	750	
	$q_{u(I)}/2_{(IASIA)}$ (Iwai)	P_f	48	1.3		743	1.060
		P_f and P_c	164	0.3	6.0	809	

P_f: Probability of failure, P_c: Consumer's risk, $C_{t(min)}$: Minimum total cost, $F_{s(min)}$: Minimun F_s

Table 6. Details of construction cost

Category	Content	Symbol	Unit cost
Individual unit cost	Construction land	C_a	0.15 (K-yen/m^2)
	Embankment work	C_b	5.3 (K-yen/m^3)
	Investigation after failure	C_{R1}	62.6 (K-yen/m)
	Land lease cost	C_{R2}	0.6 (K-yen/m)
Investigation/Test cost	Boring	C_B	24,600 (yen/m)
	Sampling	C_s	32,800 (yen/number)
	Laboratory test	C_E	5,700 (yen/specimen)
Construction cost	Initial construction work	C_c	720 (K-yen/m)
	Repair after embankment failure	C_f	783.2 (K-yen/m^2)
	Initial site investigation	C_i	0.3 (K-yen/m^3)
	Total cost	C_t	$C_c+P_fC_f+C_i$ (K-yen/m)

P_f: Probability of failure

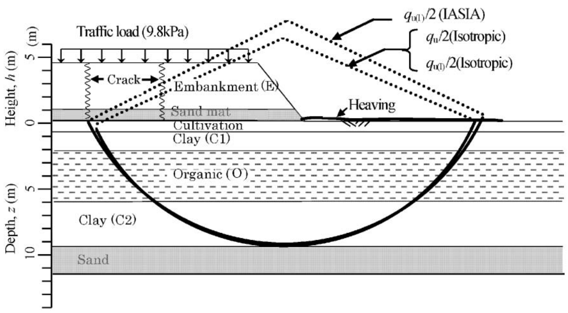

Fig. 22. The slip surfaces for the $F_{s(min)}$ of the 75-mm sampler

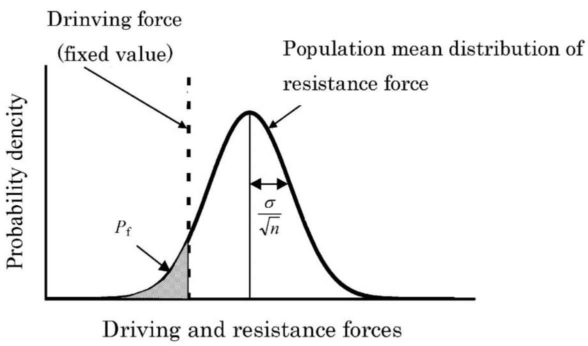

Fig. 23. The definition of the probability of failure

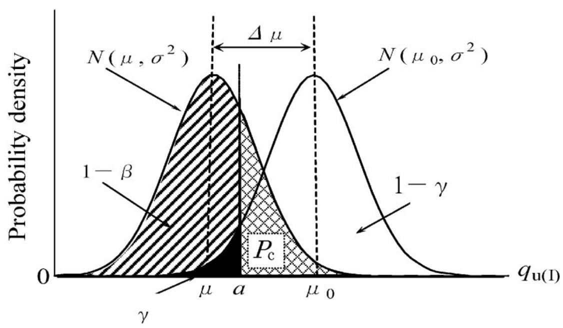

Fig. 24. The definition of consumer's risk

The ground water level is near the ground surface year round since the site used is a rice field. Therefore, the ground surface especially is not in an overconsolidation condition, as shown in Fig. 18.

Using the minimum slip surface factor for an actual failed embankment site as shown in Fig. 22, the effect of strength anisotropy on optimum embankment design is quantitatively examined from the relationships between probability of failure (P_f), consumer's risk (P_c) and number of specimen (n) for cases of the known population, as mentioned below:

i) The driving and resistance force of soil strata, except O and C_2 deposits, are derived as fixed values from the minimum slip surface safety factor (F_s).

ii) The $q_{u(I)}$ values are estimated from Shogaki's improved method (2006b). The population mean (μ) and population standard deviation (σ) for the resistance force of O and C_2 deposits are estimated from slip surface length transformation multiplied by unit width of embankment for each deposit.

iii) The resistance force distributions of O and C_2 deposits obtained from (ii) are regarded as the population mean. The confidence interval of the population mean is derived by calculating n of extracted sample and the population means distribution of total resistance force together with other fixed values. The probability in which the population mean distribution is less than that of the driving force is calculated as shown in Fig. 23 (Shogaki and Takahashi, 2007). This value is defined as P_f. The P_c is the probability in which the risk of being adopted as the strength greater than *in-situ* undrained shear strength ($q_{u(I)}$) is defined as shown in Fig. 24 (Shogaki and Takahashi, 2007). The $N(\mu_0, \sigma^2)$ is distribution of the population mean (μ_0) obtained from $q_{u(I)}$, $N(\mu, \sigma^2)$ is distribution of the population mean

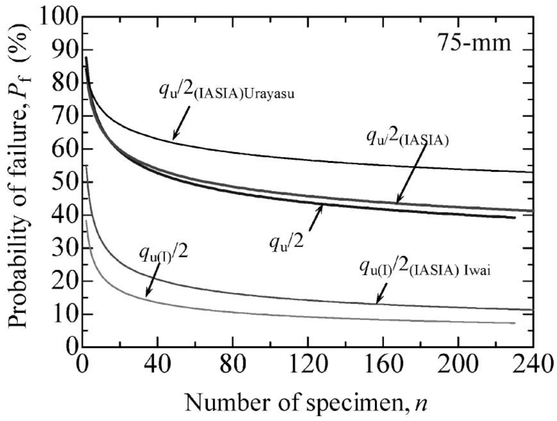

Fig. 25. The relationship between P_f and n (75-mm sampler)

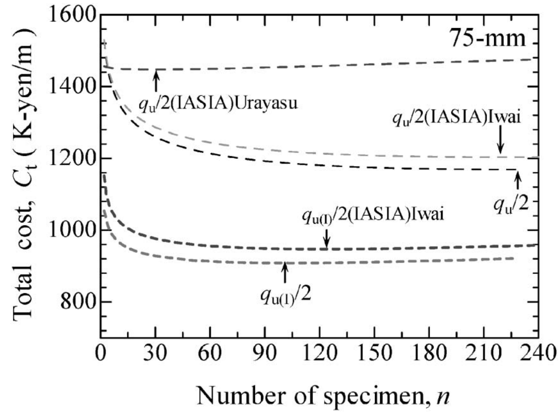

Fig. 27. The relationship between C_t and n (75-mm sampler)

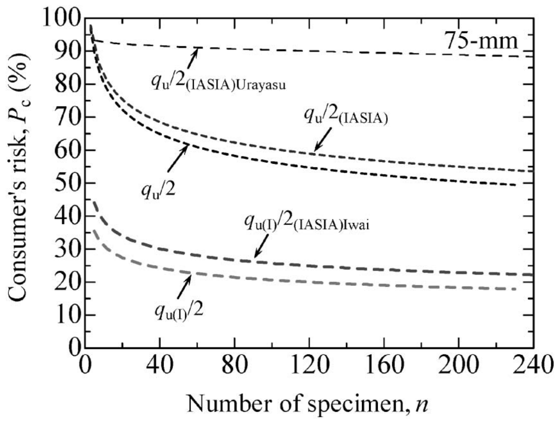

Fig. 26. The relationship between P_c and n (75-mm sampler)

(μ) of a hypothetical $q_{u(I)}$ in which the mean value is smaller as $\Delta\mu$ and σ is the lower-sided 95% confidence limit of $N(\mu_0, \sigma^2)$. In hypothesis testing of $\mu = \mu_0$, the left part (black part) of a shown in Fig. 24 is rejected by a 5% level of significance (γ). The right part is the confidence rate $(1-\gamma)$ and $\mu = \mu_0$ is adopted in hypothesis testing. Namely, P_c runs the risk of being adopted as correct if the $q_{u(I)}$ has the same lower quality as $\Delta\mu$. In practice, the adoption of this was used for the design value in the first stage of the investigation, but the embankment design reliability decreased since the risk is underestimated.

The relationships between P_f, P_c and n are shown in Figs. 25 and 26 for $q_u/2$ and $q_{u(I)}/2$ obtained from the 75-mm sampler together with those of the IASIA method for the $q_{u(I)}/2_{(IASIA)}$ of Iwai and Urayasu sites as an average example in Fig. 5 since the anisotropic strength of Iwai O and C2 soils are smaller than those of other deposits in Fig. 5. The coefficient of variation of the $q_{u(I)}/2_{(IASIA)}$ uses the same value as that of $q_u/2$. The P_f and P_c values of the $q_u/2_{(IASIA)}$ are larger than those of the $q_u/2$ value under the same n, due to strong inherent strength anisotropies using Urayasu $q_u/2_{(IASIA)}$ for the Iwai site, since the P_f and P_c values from the $q_u/2$ are $(2.5 \sim 25.5)$% and $(4.7 \sim 42.3)$% less than those of the Iwai $q_u/2_{(IASIA)}$ and Urayasu $q_u/2_{(IASIA)}$, as shown in Table 5. Therefore, the design result is underestimated by disregarding strength anisotropies.

The relationship between n and C_t, to examine the effects of P_f and P_c on n and C_t, is shown in Fig. 27 for the data of P_f and P_c in Figs. 25 and 26 to avoid complication. The construction cost details are summarized in Table 6. If P_c is not considered, the C_t value decreases with increasing n and the C_t becomes minimal ($C_{t(min)}$), as shown in Table 5. On the other hand, if P_f and P_c are considered, the C_t values increase, as shown in Table 5. However, the P_c values of the $q_u/2_{(IASIA)}$ and $q_{u(I)}/2_{(IASIA)}$ for Iwai decreases to 24.8% from 54.3% in the case of the 75-mm sampler and n increases, thus avoiding latent risks. These mean that the IASIA method and the $q_{u(I)}$ can be used for optimum embankment design based on performance provisions.

CONCLUSIONS

The conclusions obtained in this study are summarized as follows:

1) A new method for measurement of the undrained strength anisotropy was proposed by doing an unconfined compression test using small size specimens with a different angle of inclination (β) to the vertical. This method is useful because it can be measured from samples taken with the 75 mm diameter stationary piston sampler, which is widely used in Asian countries.
2) The unconfined compressive strength (q_u) decreased with the increase in the β values, and the values of $\beta = 90°$ were consistently smaller. The range of the ratios of the q_u values of specimens of $\beta = 90°$ to those of specimens with $\beta = 0°$ ($q_u(90°)/q_u(0°)$) were in the range of 0.5 to 0.9. The undrained strength anisotropy cannot be estimated by parameters such as the I_p value because of the complicated relationship with the factors influencing undrained anisotropic strength. The undrained inherent anisotropic strength of the soils in the designated area must be directly measured.

3) The ratio of $q_u/2$ to the *in-situ* undrained shear strength ($q_{u(I)}$) estimated from Shogaki's improved method (2006b) and the *in-situ* undrained shear strength ($c_{u(I)}$) measured from the CK_0UC under the *in-situ* preconsolidation pressure ($\sigma'_{p(I)}$) (Shogaki, 1996) were $(68\sim84)\%$ because of sample disturbance. The anisotropic strengths of organic (O) and soft (C2) clay were smaller than those of other deposits. In particular, for $\beta=30°$ and $60°$, the anisotropies were smaller and have isotropic behaviors for undrained shear strength (c_u). However, the q_u values of $\beta=90°$ for the O and C2 clay were 71% and 82% of those of $\beta=0°$.
4) A new method (IASIA) for slope stability analysis, taking the inherent and stress-induced anisotropy into consideration, was proposed. The minimum safety factor of the $q_u/2$, $q_{u(I)}/2$ and the IASIA method using $q_{u(I)}/2$ were 0.872, 1.016 and 1.039 at Iwai site. The slip surface coincided with the actual failed embankment. The applicability of the IASIA method was recommended from the case histories of embankment failures on soft soils.
5) The probability of failure (P_f) and consumer's risk (P_c) from the $q_u/2$ was $(2.5\sim25.5)\%$ and $(4.7\sim42.3)\%$ less than those of the Iwai $q_u/2_{(IASIA)}$ and Urayasu $q_u/2_{(IASIA)}$. Therefore, the design results were underestimated by disregarding strength anisotropies. The P_c value of $q_u/2$ was smaller than that of Iwai $q_u/2_{(IASIA)}$ since the Iwai $q_u/2_{(IASIA)}$ was smaller than q_u. If, the P_f and P_c are considered, the C_t values increased. However, the P_c values decreased to 24.8% from 54.3% in the case of the 75-mm sampler and n increased, thus avoiding latent risks. These mean that the IASIA method and the $q_{u(I)}$ can be used for optimum embankment design based on performance provisions.

NOTATION

C_t: total cost
c_u: undrained shear strength
$c_{u(I)}$: *in-situ* undrained shear strength measured from the CK_0UC under $\sigma'_{p(I)}$
E_{50}: secant modulus
F_s: safety factor
I_p: plasticity index
n: number of specimens
P_c: consumer's risk
P_f: probability of failure
q_u: unconfined compressive strength
$q_{u(I)}$: *in-situ* q_u value estimated by Shogaki's improved method
r: correlation coefficient
s: standard deviation
S_0: specimen suction
w_n: natural water content
ρ_t: wet density
α: failure angle of a specimen
β: angle of inclination to the vertical
γ: 5% level of significance
ε_f: strain at failure
σ: population standard deviation
σ_a: axial stress
σ'_p: preconsolidation pressure
$\sigma'_{p(I)}$: *in-situ* preconsolidation pressure estimated by Shogaki's method
σ_{vo}: overburden pressure
μ: population mean
μ_0: population mean obtained from $q_{u(I)}$

REFERENCES

1) Aas, G. (1965): A study of the effect of vane shapes and rate of strain on the measurement of *in-situ* shear strength of clays, *Proc. 6th ICSMFE*, **1**, 141–145.
2) Adachi, K. and Miyahama, K. (1962): Study on soft clay under embankment, *Tuchi-to-Kiso*, **10**(4), 9–16 (in Japanese).
3) Asaoka, A. and Ohtsuka, S. (1989): Coupling solutions of bearing capacity–A case study, *Proc. 12th ICSMFE*, **3**, 1709–1712.
4) Asaoka, A. and Kodaka, T. (1992): Bearing capacity of foundations on clays by the rigid plastic finite element model, *Proc. 4th Int. Symp. on Numerical Models in Geomechanics*, **2**, 839–849.
5) ASTM standards (1992): D4427–92, Standard classification of peat samples by laboratory testing, *Annual Book of ASTM Standards*, **4**(8), 767–768.
6) Bishop, A. W. (1966): The strength of soils as engineering materials, *Géotechnique*, **16**(2), 89–130.
7) Bjerrum, L. (1973): Problems of soil mechanics and construction on soft clay, *Proc. 8th ICSMFE*, **3**, 109–159.
8) Casagrande, A. and Carilo, N. (1944): Shear failure of anisotropic soils, *Contribution to Soil Mechanics*, ASCE, 1941–1953.
9) Davis, E. H. and Christian, J. T. (1971): Bearing capacity of anisotropic cohesive soil, ASCE, **97**(SM5), 753–768.
10) Duncan, J. M. and Seed, H. B. (1966a): Anisotropy and stress reorientation in clay, ASCE, **92**(SM5), 21–50.
11) Duncan, J. M. and Seed, H. B. (1966b): Strength variation along failure surfaces in clay, ASCE, **92**(SM5), 81–104.
12) Hansen and Gibson (1949): Undrained shear strengths of anisotropically consolidated clays, *Géotechnique*, **1**(3), 189–204.
13) Hanzawa, H. and Tanaka, H. (1992): Normalized undrained strength of clay in the normally consolidated state and in the field, *Soils and Foundations*, **32**(1), 132–148.
14) Hanzawa, H. (1995): Application of direct shear test results to practice, *Proc. Japanese Sympo. on Method and Application of Direct Shear Test*, 87–94 (in Japanese).
15) Hvorslev, M. J. (1960): Physical components of the shear strength of saturated clays, *Proc. Res. Conf. on Shear Strength of Cohesive Soils*, 169–273.
16) Japan Highway Public Corporation (1966): *Report of the Construction of Test Embankment in Aikoh* (in Japanese).
17) Japan Highway Public Corporation (1977): *Report of the Construction of Test Embankment in Iwamizawa* (in Japanese).
18) Japanese Geotechnical Standards (1996): Method for K_0 consolidate-undrained triaxial compression test on soils with pore water pressure measurement, (JGS 0525–1996), 349–358 (in Japanese).
19) Japanese Geotechnical Society (2004): Method for obtaining soil samples using thin-walled tube sampler with fixed piston (JGS 1221–2003), *Standard of Japanese Geotechnical Society for Soil Sampling-Standards and Explanations-*, 1–7.
20) Japanese Geotechnical Society (2006): The manual for unconfined compression test with suction measurement, *Proc. Miniaturization, Accuracy and Design Reliability for Geotechnical Investigations and Lab Tests*, Appendix, 1–14 (in Japanese).
21) Japanese Standard Association (1993): Test method for one-dimensional consolidation properties of soils, *JIS A 1217–1990*, 1–13 (in Japanese).

22) JSSMFE (1990): *Engineering of Organic Soils*, Japan Society of Soil Mechanics and Foundation Engineering, 103–212 (in Japanese).
23) Ladd, C. C., Foott, R., Ishihara, K., Scholosser, F. and Poulos, H. G. (1977): Stress-deformation and strength characteristics, *Proc. 9th ICSMFE*, **2**, 421–494.
24) Lo, K. Y. (1965): Stability of slopes in anisotropic soils, ASCE, **91**(SM4), 85–106.
25) Matsuo, M. and Asaoka, A. (1976): A statistical study on a conventional, Safety factor method, *Soils and Foundations*, **16**(1), 75–90.
26) Matsuo, M. and Shogaki, T. (1988): Effect of plasticity and disturbance on statistical properties of undrained strength, *Soils and Foundations*, **28**(2), 14–24.
27) Mesri, G. (1989): A reevaluation of $s_u(mob) = 0.22\ \sigma'_p$ using laboratory shear test, *Canadian Geotechnical Journal*, **26**(1), 162–164.
28) Mikasa, M., Tanaka, N. and Ohshima, A. (1987): *In-situ* strength anisotropy of clay by direct shear test, *Proc. 8th Asian Regional Conf. on SMFE*, **1**, 61–64.
29) Muromachi, T. and Watanabe, S. (1962): Deformation soft peat foundation under embankment, *Railway Technical Research Report*, (154) (in Japanese).
30) Sekiguchi, H. and Ohta, H. (1977): Induced anisotropy and time dependency in clays, *Proc. Specialty Session 9, 9th ICSMFE*, 229–238.
31) Shogaki, T. (1996): A method for correcting consolidation parameters for sample disturbance using volumetric strain, *Soils and Foundations*, **36**(3), 123–131.
32) Shogaki, T. (2006a): Microstructure, strength and consolidation properties of Ariake clay deposits obtained from samplers, *Journal of ASTM International*, **3**(7), 98–105.
33) Shogaki, T. (2006b): An improved method for estimating *in-situ* undrained shear strength of natural deposits, *Soils and Foundations*, **46**(2), 1–13.
34) Shogaki, T. (2007): Effects of size on unconfined compressive strength properties of natural deposits, *Soils and Foundations*, **47**(1), 119–129.
35) Shogaki, T. and Matsuo, M. (1985): Factor analysis approach to unconsolidated undrained shear strength of clay with some consideration on microscopic structures, *Proc. Sympo. on Sampling*, 109–116 (in Japanese).
36) Shogaki, T., Moro, H. and Sudoh, T. (1995a): Statistical properties of soil date within thinwalled samplers, *Proc. Sympo. on a Method for the Limit State Design of the Foundation Construction*, 193–200 (in Japanese).
37) Shogaki, T., Moro, H., Mihara, M. and Kaneko, M. (1995b): Effect of sample disturbance on consolidation parameters of anisotropic clay, *Proc. Int. Sympo. on Compression and Consolidation of Clayey Soils*, 561–566.
38) Shogaki, T. and Moro, H. (1996): A method for stability analysis of slopes in anisotropic soils, *Proc. 7th International Symposium on Landslides*, **1**, 1357–1362.
39) Shogaki, T., Moro, H. and Matsuo, M. (1998): Case histories for settlement analysis in ground improved by vertical drain, *Proc. 4th Int. Conf. on Case Histories in Geotechnical Engineering*, 972–977.
40) Shogaki, T. and Nochikawa, Y. (2004): Triaxial strength properties of natural deposits at K_0 consolidation state using a precision triaxial apparatus with small size specimens, *Soils and Foundations*, **45**(2), 41–52.
41) Shogaki, T, and Sakamoto, R. (2004): The applicability of a small diameter sampler with a two-chambered hydraulic piston for Japanese clay deposits, *Soils and Foundations*, **44**(1), 113–124.
42) Shogaki, T., Sakamoto, R., Kondo, E. and Tachibana, H. (2004a): Small diameter cone sampler and its applicability for Pleistocene Osaka Ma12 clay, *Soils and Foundations*, **44**(4), 119–126.
43) Shogaki, T., Sakamoto, R., Kanno, Y., Kobayashi, H. and Momose, S. (2004b): Standard penetration test sample quality, *IS-Osaka*, 159–164.
44) Shogaki, T. and Takahashi, A. (2007): Proc. Reliability of the cone penetration, undrained shear strength tests and the optimum embankment design method, *The 13th Asian Regional Conf. on SMGE*, 1085–1088.
45) Skempton, A. W. (1948): A study of the immediate triaxial test on cohesive soils, *Proc. 2nd ICSMFE*, **1**, 192–196.
46) Skempton, A. W. (1954): The pore-pressure coefficients A and B, *Géotechnique*, **4**, 143–147.
47) Tanaka, H., Sharma, P., Tsuchida, T. and Tanaka, M. (1996): Comparative study on sample quality using several types of samplers, *Soils and Foundations*, **36**(2), 57–68.
48) Tsuchida, T., Mizukami, J., Oikawa, K. and Mori, Y. (1989): New method for determining undrained strength of clayey ground by means of unconfined compression test and triaxial test, *Report of the Port and Harbor Research Institute*, **28**(3), 81–145 (in Japanese).
49) Yamamoto, M. and Hoshi, T. (1967): Engineering properties of peaty ground as an embankment foundation, *J. of Road*, **11**, 45–55 (in Japanese).